A ligand-independent fast function of RARα promotes exit from metabolic quiescence upon T cell activation and controls T cell differentiation

L.R. Friesen[1,2], **B. Gu**[3], **C.H. Kim**[1,2,4]

[1]Department of Pathology, University of Michigan School of Medicine, Ann Arbor, MI 48109

[2]Mary H. Weiser Food Allergy Center, University of Michigan School of Medicine, Ann Arbor, MI 48109

[3]Department of Comparative Pathobiology, Purdue University, West Lafayette, IN 47906

[4]Rogel Cancer Center, University of Michigan School of Medicine, Ann Arbor, MI 48109

Abstract

Vitamin A metabolites play important roles in T cell activation and differentiation. A conventional model of RARα function relies upon retinoic acid (RA)-liganded RARα binding to specific DNA motifs to regulate gene expression in the nucleus. However, this genomic function fails to explain many of the biological responses of the RA-RARα axis on T cells. We generated a mouse line where RARα is over-expressed in T cells to probe RARα function with unprecedented sensitivity. Using this model together with mice specifically lacking RARα in T cells, we found that RARα is required for prompt exit from metabolic quiescence in resting T cells upon T cell activation. The positive effect of RARα on metabolism is mediated through PI3K and subsequent activation of the Akt and mTOR signaling pathway. This largely non-genomic function of RARα is surprisingly ligand-independent and controls the differentiation of effector and regulatory T cell subsets.

Introduction

Resting T cells maintain metabolic and functional quiescence, but upon antigenic stimulation, they rapidly exit quiescence to undergo the activation process [1, 2, 3]. Integrated signals from cytokine receptors, T cell receptors (TCR), co-stimulatory molecules, and nutrient uptake increase T cell metabolism [4, 5]. Increased cellular metabolism is necessary to supply energy and building blocks for cell growth, leading to cell proliferation and differentiation [6]. Key pathways that trigger T cell metabolism and enlargement during activation include the phosphatidylinositide-3 kinase (PI3K), protein kinase B (Akt), and

mammalian target of rapamycin (mTOR) pathway [7, 8, 9, 10]. This pathway is activated upon triggering of TCR and costimulatory molecules [8, 11, 12]. Metabolites and nutrients, such as amino acids and short-chain fatty acids, also activate the pathways [13, 14].

The vitamin A metabolite all-trans retinoic acid (RA) and its receptor retinoic acid receptor α (RARα) profoundly regulate the migration and differentiation of T cells. RA suppresses Th17 and Th9 cell differentiation but induces FoxP3 expression for Treg generation [15, 16, 17, 18, 19, 20, 21]. Other T helper cell subsets, such as Th1 and Th2, are also affected but in a more obscure manner compared to Th17 and Treg cells [22, 23, 24]. Beyond T cell polarization, RA induces upregulation of chemokine receptor CCR9 and integrin α4 to generate gut-homing cells and induces P2X7 and Art2b for pyroptosis-mediated negative regulation [25, 26, 27, 28]. It is the dogma that RARα, the major mediator of the biological effects of RA, functions through transcriptional regulation in the nucleus [29], which is also referred to as the conventional genomic function of RARα.

However, the genomic function fails to explain rapid biological effects of RARα, such as chemotaxis of neurite cells, platelet activation, and activation of PI3K [30, 31, 32], as well as apparently RARE-independent gene regulation in many cell types [22, 33, 34]. It has been reported that RARα exerts non-genomic function in non-immune cells such as neuroblastoma and fibroblast cells, where some RARα molecules are present in the cytoplasm or cell membrane in lipid rafts and interact with the p85 subunit of class I PI3K, Akt and Gαq proteins [35, 36]. Class I PI3Ks, typically activated by G-protein coupled receptors and tyrosine kinase receptors, generate phosphatidylinositol (3,4,5)-trisphosphate $(PI(3,4,5)P_3$ or $PIP_3)$, which activates Akt, PDK1, and Btk1 via pleckstrin homology domain (PH domain) [37]. For T cells, RARα is required for fast signaling and activation of T cells and their differentiation to Th1 cells during *Toxoplasma Gondii* infection via a largely unknown mechanism [38]. Thus, there is a need to establish non-genomic roles of RARα in T cells and the immune system as a whole.

We generated a mouse line to probe the function of RARα with increased sensitivity and investigated the function of RARα in regulating T helper cells with the focus on fast acting non-genomic roles. We report here that RARα functions to vigorously increase the activation of the PI3K/Akt/mTOR signaling pathway upon TCR stimulation, inducing prompt exit from the naïve state metabolic quiescence and leading to the elevated state of metabolism. This, in turn, profoundly influences the T cell differentiation process, leading to increased generation of Th17 cells. Importantly, the RARα ligand, RA, negatively regulates the non-genomic function potentially by shifting their function to conventional nuclear functions. Our findings establish a ligand-independent function of RARα in regulating T cell metabolism and differentiation.

Results

Generation and characterization of RARα-Tg versus Rara*LCK* mice

To generate an effective tool to probe RA-RARα functions, we generated mice where RARα is over-expressed specifically in T cells utilizing a human CD2 promoter (Figure 1a). We also generated mice deficient in RARα expression by crossing Rara (flox/flox) mice to

Lck-Cre mice. These mice produce CD4 T cells with increased or decreased RARα activity as measured by a RARE-reporter assay (Figure 1b). We assessed how T-cell specific overexpression or loss of RARα affects T cell populations in the steady state. The Rara^{LCK} and RARα-Tg mice had overall no significant defect in thymocyte populations. Both strains had a slight decrease in the CD4$^+$CD8$^+$ double positive population with small compensatory increases in both CD4$^+$ and CD8$^+$ single positive populations (Figure S1a). T helper cell numbers were not affected in the spleen, mesenteric lymph node (MLN), or large intestine lamina propria (Figure S1b). However, the numbers of total CD4$^+$ cells, Th17 cells, Th1 cells, but not Tregs, were decreased in the small intestine of Rara^{LCK} mice. RARα-Tg mice had increased numbers of Th17 cells in the large intestine and moderate increases of Treg numbers in MLN. Thus, intestinal T helper cell deficiency and increased numbers of colonic Th17 cells respectively are the defining features of the steady state immune system of Rara^{LCK} and RARα-Tg mice.

RARα expression supports TCR activation-induced cell enlargement and mitochondrial biogenesis

In order to determine the dose effect of RARα expression on T cell activation, naïve CD4$^+$ T cells from WT, Rara^{LCK}, and RARα-Tg mice were activated with anti-CD3 and anti-CD28 in a Th17 polarization condition. At 24h of activation, RARα-Tg T cells were significantly larger than WT and Rara^{LCK} T cells (Figure 1c, d). Also increased was the mitochondrial mass in the RARα-Tg T cells compared to WT and Rara^{LCK} T cells (Figure 1e). Cell proliferation was assessed with carboxyfluorescein succinimidyl ester (CFSE) staining at 48h in a Th17-polarizing condition. Increased proliferation of RARα-Tg T cells and decreased proliferation of Rara^{LCK} T cells were observed (Figure 1f). Cell cycle analysis revealed that Rara^{LCK} T cells had decreased, while RARα-Tg T cells had increased frequency of cells in S and G2/M phases (Figure 1g). The positive effect of RARα on CD4$^+$ T cell proliferation was detected broadly in non-polarized, Treg and Th17 culture conditions (Figure S2).

The differences in cell size and proliferation upon T cell activation indicate potential differences in cell metabolism. We found that glucose uptake was increased in the RARα-Tg but decreased in Rara^{LCK} T cells (Figure 2a). Moreover, RA suppressed the glucose uptake in RARα-Tg T cells. The mRNA expression of selected key nutrient transporters or metabolizing enzymes, such as *Glut1* (glucose), *Lat1* (amino acids), and *Glud1* (a mitochondrial glutamate dehydrogenase 1) was examined to gain more insights. In general, the expression of these transporters was higher in RARα-Tg than WT T cells cultured for 24h in a Th17 polarization condition (Figure 2b). Rara^{LCK} T cells has decreased expression of *Glut1* compared to WT T cells. RA decreased the expression of *Glut1, Glud1,* and *Lat1* in RARα-Tg T cells, but the effect on Rara^{LCK} T cells was mixed or unclear. Also measured was *Icos*, which is expressed in activated T cells to induce mTOR activation, glucose transport, glycolysis, and lipogenesis [39, 40]. RARα increased but RA suppressed *Icos* expression (Figure 2b).

RARα is required for the rapid rise of cellular metabolism during TCR activation

One of the key functions of TCR activation is to exit metabolic quiescence and increase T cell metabolism to support T cell proliferation and differentiation [3]. We measured time-dependent changes in extracellular acidification rate (ECAR) and oxygen consumption rate (OCR) upon activation of naïve WT, $Rara^{LCK}$, and RARα-Tg T cells. The activation increased ECAR and OCR (Figures 2c,d; S3a,b). The dose of RARα expression positively correlated with the increase in ECAR (ECAR) upon stimulation, while changes in OCR (OCR) were not significantly different at this early time point during T cell activation (Figures 2c,d; S3a,b). There was no difference in the basal ECAR and OCR before activation of the naïve T cells from the three mouse strains (Figure S3c). We also measured mitochondrial respiration activity for 24h-activated naive CD4$^+$ T cells. RARα-Tg T cells reached higher basal and maximum respiration levels with greater spare capacity, while $Rara^{LCK}$ T cells had reduced rates compared to WT (Figure 2e, f). The basal ECAR in these 24h-activated cells also correlated with RARα expression level. RA had a clear negative effect on these metabolic indices in RARα-Tg T cells. A similar negative effect of RA was observed for WT CD4$^+$ T cells without reaching statistical significance. These results identify a role of RARα in boosting T cell metabolism upon T cell activation.

RARα expression licenses optimal activation of Akt and mTOR in T helper cells

Cellular metabolism is controlled by the activation of the mTOR pathway, which senses and integrates TCR, nutritional, and cytokine signals to set cellular metabolic rates [41]. Akt kinases phosphorylate Tsc2 to relieve its suppressive activity on mTORC1 kinase [42]. We found that RARα-Tg CD4$^+$ T cells had higher Akt1/2/3 phosphorylation (S473) after 15 min of TCR activation (Figure 3a). In contrast, $Rara^{LCK}$ T cells had lower phosphorylation of Akt, and RA was suppressive of the Akt activation in WT and RARα-Tg cells, but not $Rara^{LCK}$ T cells. We also determined the phosphorylation of Akt (T308, a target site for PDK1) by western blotting. RARα expression also positively correlated with the phosphorylation of Akt (Figure 3b). Because PTEN down-regulation can also increase PIP$_3$ level, we examined PTEN expression. PTEN expression was not altered by RARα or RA (Figure 3b).

RA was effective at suppressing the activation of ribosomal S6 protein (phosphorylation at S235/236) in WT and RARα-Tg T cells, which was measured at 48h of activation (Figure 3c). In contrast, $Rara^{LCK}$ T cells had low phosphorylation of rS6 with no effect of RA. The increased mTOR activation in RARα-Tg T cells, together with the suppressive effect of RA, was also detected at earlier time points (Figure 3d). We also determined the phosphorylation of S6K (T421/S424, a target site for ERK) by western blotting. RARα expression positively correlated with the phosphorylation of S6K (Figure 3e). Overall, these results establish the ligand-independent role of RARα in activating Akt and mTOR in T cells, which is in line with the increased metabolism in RARα-Tg T cells.

RARα associates with PI3K for activation, which is restrained by RA

Akt is activated by PIP$_3$, which is produced by PI3K, and we examined the possibility that RARα closely associates with PI3K for functional interactions in T cells. We performed a proximity ligation assay (PLA) [43] and found that RARα closely associates with the p85

subunit of PI3K, with reduced interaction in the presence of RA (Figure 4a, b). We also detected PI3K activity in T cells by observing membrane localization of a PIP_3-sensing reporter protein made of the PH domain of Akt1 (GFP-PH^{Akt}). Upon TCR stimulation, PIP_3 localization to the cell membrane was increased in RARα-Tg T cells compared to WT cells (Figure 4c, d). $Rara^{LCK}$ T cells had lower membrane PIP_3 activity. RA had negative effects on RARα-associated membrane PIP_3 localization. Thus, the non-genomic function of RARα in activating the PI3K and Akt pathways is not only ligand-independent but is also negatively regulated by the ligand. A ligand-binding defective (LB) mutant form of RARα had increased localization to the non-nuclear/cytoplasmic compartment, and RA failed to affect its localization (Figure 5b,c).

RARα supports Th17 but limits Treg and Th1 differentiation *in vitro*

Because increased levels of PI3K, Akt, mTOR, and metabolic activities support Th17 cell differentiation and inhibit Treg differentiation [1, 9, 44], we examined the possibility that increased expression or activity of RARα favors the differentiation of Th17 over that of Treg cells. The effects of RA in suppression of Th17 differentiation and induction of Treg differentiation were high in RARα-Tg cells but absent in $Rara^{LCK}$ cells (Figure 6a, S4a, b). Gain of RARα expression enhanced Th17 differentiation but suppressed Treg differentiation. Conversely, loss of RARα expression enhanced Treg differentiation but suppressed Th17 differentiation. We also found that RA dampens the function of RARα in supporting Th17 cells. In contrast, the negative effect of RARα dose on Treg generation was switched to a positive one by RA. In contrast, Th1 differentiation was increased in $Rara^{LCK}$ cells and decreased in RARα-Tg cells, with slight positive effects of low concentrations of RA in WT and Tg cells (Figure 6c, S4c). We used charcoal stripped FBS in culture media to minimize any effects of RA on the function of RARα. Ro41–5253, a RARα antagonist, did not affect Th17, but slightly suppressed, Treg, differentiation in WT and RARα-Tg cells (Figure S5), indicating very low levels of RA in this culture condition. We also examined the master transcription factors such as RORγt and T-bet in CD4 T cells cultured in Th17 and Th1 polarization conditions. Dose-dependent downregulation of RORγt in theTh17 polarizing condition and upregulation of T-bet expression by RA in both Th17-and Th1 polarizing conditions in WT and RARα-Tg cells, but not $Rara^{LCK}$ cells, were observed (Figure S6a,b). These results reveal ligand-independent functions of RARα in regulating Th differentiation in RA-deficient conditions before further regulation by RA. Its positive impact on Th17 differentiation is particularly interesting.

The regulatory effect of RARα in T cell differentiation is mediated by activation of Akt and mTOR

To assess whether the signaling defect of $Rara^{LCK}$ cells was due to simple loss of RARα or potential defects in other functions, we restored WT or ligand-binding defective (LB, G303E) RARα expression in these cells by retroviral expression. Restoration of RARα in $Rara^{LCK}$ cells increased Th17 differentiation, and WT RARα also restored the sensitivity to RA (i.e. suppression of Th17 polarization by RA) (Figure 6d). Restoration of RARα by retroviral expression also decreased Treg differentiation without increasing the sensitivity to RA (Figure 6e). This is likely due to the need for RARα at early stage of Treg differentiation, but retroviral expression takes at least 36h to restore FoxP3 expression.

Restoration of RARα expression in Rara^{LCK} cells increased the activation (phosphorylation at S473) of Akt and rS6 (S235/236) in the absence of RA, and the addition of RA suppressed this effect in T cells with enforced expression of WT RARα. However, LB RARα (a mutant form of RARα lacking ligand binding capacity) [45], while it increased the activation of Akt and rS6, failed to confer the sensitivity to RA as expected (Figure 6f; S7a, b).

To determine if forced activation of Akt signaling would mimic the function of RARα in increasing mTOR activation and alter T cell differentiation, a constitutively active form of Akt (myristoylated Akt) was expressed in Rara^{LCK} cells, and the phosphorylation of rS6 was assessed (Figure 6g). The constitutively active Akt signaling led to increased rS6 phosphorylation and Th17 differentiation but decreased Treg differentiation (Figure 6h; S8a,b). In this condition, RA was able to neither decrease rS6 phosphorylation and Th17 polarization nor increase Treg differentiation. Inhibition of PI3K signaling pathways with CAL-101 (PI3K catalytic subunit p110δ), LY294002 (PI3Kα, PI3Kδ, and PI3Kβ), and IC-87114 (PI3Kδ) suppressed Th17 differentiation (Figure S9a), indicating the importance of PI3K in the process. Rapamycin, which inhibits the mTOR pathway, also decreased Th17 and Th1 differentiation and increased Treg differentiation (Figure S9b). These results indicate that the modulatory effect of RA is mediated, in part, by suppressing the Akt-mTOR activating function of RARα. Overall, these results establish a mechanism for RARα-mediated regulation of T cell activation and differentiation.

RARα promotes Th17-mediated intestinal inflammation

To determine the RARα dose effect on Th17 generation *in vivo*, we transferred naïve CD4$^+$ T cells, isolated from WT, Rara^{LCK}, and RARα-Tg mice, into Rag1$^{-/-}$ mice. RARα-Tg T cells induced rapid colitis as indicated by body weight loss (Figure 7a), colon shortening (Figure 7b) and histological changes (Figure 7c), whereas Rara^{LCK} T cells failed to induce inflammatory responses. The T cell profile at the endpoint indicated that higher RARα dose induced the generation of higher percentages and absolute numbers of Th17 cells in MLN, and colonic lamina propria (Figure 7d). In contrast, Rara^{LCK} T cells were inefficient in becoming Th17 cells in the MLN and large intestine of the Rag1$^{-/-}$ mice, consistent with their low colitogenic effect. The percentages of Th1 and Treg cells were less affected, with increased percentages of MLN Tregs in the RARα-Tg group and increased percentages of Th1 cells in the Rara^{LCK} group, the latter of which is in line with the *in vitro* differentiation data (Figure 6c). These results demonstrate *in vivo* effects of RARα in regulating Th cell responses, particularly the positive effect on inflammatory Th17 cells.

Discussion

While long known as a nuclear transcription factor, the quick function of RARα in regulating T cells has not been explained well with just its transcriptional regulatory function. More specifically the RARα-associated increases in cell signaling pathways, metabolism, and proliferation, shown in this study, are not easily explained by the function of RARα as a transcription factor. We investigated the mechanism for the non-genomic or largely non-transcriptional effect of RARα in T helper cells. We found that unliganded

RARα has a novel function in activating T cell signaling and metabolism through activation of PI3K, Akt, and mTOR. This function of RARα induces T cell exit from the metabolic quiescence to achieve active metabolism in a prompt manner upon T cell activation. We also provided evidence that this unconventional function of RARα has significant impacts on the differentiation and effector function of T helper cells.

We created and utilized animal models with which we can probe the impact of RARα on T cell metabolism and differentiation with unprecedentedly high sensitivity. A striking positive effect of the increased RARα expression was observed on T cell size and proliferation. Proliferation of T helper cells *in vitro* was enhanced, regardless of the polarization condition. Along with the larger cell size, RARα promoted mitochondrial biogenesis, which indicates that cellular metabolism is also increased. Metabolic pathways utilized by T helper cells include glycolysis and mitochondrial oxidative phosphorylation, which are increased upon TCR stimulation and necessary to support T cell differentiation. Particularly, Th17 cell differentiation requires glycolysis, whereas Treg differentiation depends on relatively more oxidative phosphorylation [44, 46]. RARα increases both oxidative phosphorylation and glycolysis in T cells. This property can favor the generation of Th17 cells over Tregs, and our results indeed support the role of RARα-induced metabolism in inducing Th17 cells. In contrast, the ligand-independent function of RARα appears to dampen Th1 polarization, while the presence of RA positively affects Th1 differentiation. Basal levels of metabolism in unstimulated naïve T cells, both ECAR and OCR, were unchanged by the expression of RARα. It is during T cell activation when RARα effectively promotes T cell metabolism and proliferation, which can facilitate exit from metabolic quiescence [47]. On the other hand, RA shifts liganded RARα away from cytoplasmic to nuclear functions for gene expression. By doing so, RA reigns in metabolic activity and promotes iTreg differentiation. These results not only provide novel information beyond previously described roles of RA in regulating T cell differentiation, but also provide mechanisms for the rather enigmatic RA-regulated polarization of Th17 cells and Tregs [15, 26].

The rapid effect on T helper cell metabolism during TCR activation is well explained by the effects of RARα on signaling pathways. The mTOR signaling pathway uses environmental cues, such as TCR signaling, co-stimulation, cytokines, and nutrients to invoke changes to cellular functions including metabolism, proliferation, autophagy, and differentiation [41]. The activity of mTORC1, assessed with rS6 phosphorylation status in our study, indicates that the mTOR pathway is bidirectionally regulated by RARα and RA. RARα increases mTOR activity, while RA (i.e. liganded RARα) suppresses it. Activation of the mTOR pathway by Akt signaling occurs following T cell activation [48]. Our results show that the activation of Akt signaling pathway is increased by unliganded RARα and this is suppressed by RA (or liganded RARα). Akt activation following TCR stimulation is mediated by PI3K. PI3K is recruited to the TCR activation complex via the protein, called linker for activation of T cells (LAT) [49]. PI3K generates PIP_3, which attracts Akt and PDK. PDK1 phosphorylates Akt, which dissociates from the plasma membrane and phosphorylates downstream substrates such as TSC2 and Foxo1 among many molecules [50]. Our PLA data indicate that RARα can associate with PI3K in T cells, and this is negatively regulated by RA. The physical association between RARα and PI3K has been previously determined by other techniques in neuroblastoma cells [31]. Taken together, our results support the role of RARα in activating

the signaling cascade from PI3K to Akt and subsequent activation of the mTOR pathway, which is key to increase T cell metabolism to exit metabolic quiescence.

A rather surprising finding was the ligand-independent nature of the RARα function in supporting the signaling pathway to boost cellular metabolism, and RA is suppressive on the non-genomic function. Our data indicate that the non-genomic function of RARα is expected to be present largely outside of the nucleus in locations including the cellular membrane and cytoplasm. More biochemical studies are required to establish detailed molecular association between RARα and other signaling molecules. Activation of additional signaling events downstream of PI3K activation in the nucleus is plausible. Liganded RARα is more directed to DNA binding and transcription regulation than activating PI3K. RA binding to RARα weakens the non-genomic function of RARα and this is likely to be mediated by shifting liganded RARα to the nucleus, decreasing their functions in extranuclear compartments. However, in other cell types such as platelets and neuronal cells [30, 31, 32, 35, 36], RA boosts the non-genomic functions. Therefore, the suppressive function of RA appears to be unique to T cells. Because RA induces gene expression via liganded RARα in the nucleus, it is expected that there is a shift from non-genomic to genomic function depending on RA concentrations. In low RA conditions or tissues, high levels of non-genomic action of RARα are expected. In high RA levels, the non-genomic function is minimized with the increased genomic action of liganded RARα. This mode of regulation provides a sophisticated mechanism to regulate T cell metabolism and gene expression depending on RA conditions.

A question of interest is where and when the observed function of RARα operates in regulating T cell activation, metabolism, and differentiation in physiological conditions *in vivo*. RA levels are highly heterogenous in different tissues throughout the body. RA gradients are important cues during embryogenesis. It is expected that similar but different gradients are expected to be formed in different tissues. For example, the intestine has high RA levels of RA with high levels of RA-producing RALDH1 and RALDH2 expression [25, 51], whereas skin appears to have low levels of RA based on the presence of langerin[+] DCs, which are suppressed by RA [52]. Moreover, the steady state RA levels are altered in inflammatory conditions. For example, increased CYP26A1 expression, a condition to decrease RA levels, was reported in inflamed intestine [53]. Thus, the observed function of RARα in regulating T cell metabolism and differentiation can be active *in vivo* in both RA-low and high conditions. In low RA conditions, RARα promotes T cell metabolism and Th17 cell differentiation and this function would be reduced in high RA conditions, favoring Tregs and Th1 cells.

The negative effect of RARα on Th1 differentiation was clear only in a low RA condition created by medium containing charcoal stripped FBS. We purposely used a culture medium containing charcoal-stripped FBS to study the effect of RARα in a low RA condition. Regular FBS medium is estimated to contain ~0.5 nM of RA which is still significant enough to affect Th1, Treg, and Th17 differentiation (Figure 6a–c). This culture method allows us to detect the function of RARα in negatively regulating Th1 differentiation but positively Th17 differentiation without high levels of RA effects. When RA was added to this condition, the function of RARα was altered to positively regulate Th1 cells. So

increased Th1 differentiation is due to the RARα function in medium to high RA conditions, which is in line with a previous report by Hall et al [38]. However, at low RA conditions, RARα suppressed Th1 but increased Th17 cell polarization, which is one of unique observations made in this study. Mechanistically, mTOR activation alone does not explain the functions of RARα and RA. We speculate that the impact of RARα and RA on gene expression is likely to play a role on top of the non-genomic function of RARα. This should be validated in a future study.

In this study, we found that RARα is required to rapidly increase T cell metabolism upon T cell activation, which promotes metabolic quiescence exit to support T cell proliferation and differentiation. The balance between the non-genomic and genomic effects of RARα is likely to determine the overall impact of RARα on T cell activation, metabolism and differentiation, explaining the increased Th17 cell differentiation in low RA conditions and the increased expression of FoxP3 at high RA conditions. We further determined the impact of the non-genomic function of RARα *in vivo* and demonstrated the potential of this function to induce proliferation of inflammatory Th17 cells. This highlights the important role of RARα in promoting certain effector T cell responses. Overall, we found a fast-acting RARα-dependent mechanism to promptly boost metabolism and regulate T cell differentiation upon T cell activation, the levels of which are further controlled by RA levels.

Materials and Methods

Mice

Mice that over-express mouse RARα specifically in T cells were created utilizing a human CD2 promoter. Mouse RARα cDNA was cloned into the CD2 transgenic expression vector [54]. A SalI/XbaI fragment containing the transgene was used to generate C57BL/6 transgenic mice at the Transgenic Mouse Core Facility at Purdue University. A high transgene-expressing mouse line was established. C57BL/6 mice (stock #002216), distal *Lck*-cre mice (stock #012837), RARα-flox mice (a gift from Dr Chambon, Institut de Génétique et de Biologie Moléculaire et Cellulaire, France) [52, 55], and *Rag1*^{−/−} C57BL/6 mice (stock #002216) were purchased from the Jackson Laboratory (Bar Harbor, ME). The *Lck*-cre mice were mated with floxed mice to generate the T cell specific Rara[LCK] mice strain. Primers used for genotyping PCR are described in Supplemental Table 1. Mice, maintained in a specific pathogen-free condition, were generally 6–8 weeks of age when used for experiments. Littermate mice with flox/flox genotype without Cre gene or without the transgenic gene were used as the control mice. Animal protocols were approved by the Animal Care and Use Committees at University of Michigan and Purdue University.

Cell isolation and culture

Naïve T cells were magnetically isolated with the Naïve CD4^{+} T cell Kit (Miltenyi Biotec, Somerville, MA). For *in vitro* culture, cells were cultured in complete RPMI-1640 media containing charcoal stripped FBS (Gibco™). Plate-bound anti-CD3 (5 μg/mL; clone 145–2C11) and anti-CD28 (2 μg/mL; clone 37.51) were used for activation *in vitro* with cytokines according to indicated culture conditions. For nonpolarized (Tnp) culture, hIL-2 (100 U/mL) was added. For Th17-polarizing culture, cytokines and neutralizing antibodies

included mIL-6 (20 ng/mL), mIL-1β (10 ng/mL), mIL-21 (10 ng/mL), mIL-23 (10 ng/mL), mTNFα (5 ng/mL), hTGFβ−1 (5 ng/mL), anti-IFNγ (10 μg/mL, clone XMG1.2), and anti-IL-4 (10 μg/mL, clone 11B11). For the Treg-polarizing culture, hIL-2 (100 U/mL) and hTGFβ−1 (0.2 to 1 ng/mL) were added. For Th1-polarizing culture, hIL-2 (100 U/mL), mIL-12 (10 ng/mL), anti-IL-17A (10 μg/mL, clone 17F3), and anti-IL-4 (10 μg/mL) were used. Cytokines were purchased from BioLegend (San Diego, CA), and neutralizing antibodies were purchased from BioXcell (Lebanon, NH). Cells were cultured in the presence of all-trans retinoic acid (RA; 10 nM unless otherwise specified; Sigma Aldrich; St. Louis, MO) or Ro41–5253 (100 nM; Sigma Aldrich) at the time of culture as indicated. For inhibitor studies, rapamycin (5 and 25 nM), CAL-101 (1 and 10 nM), LY294002 (2 and 10 nM), and IC-87114 (2 and 10 nM) were added on day 0 and 2; all inhibitors were from Cayman Chemical (Ann Arbor, MI).

Flow cytometric analysis of surface and intracellular antigens

Surface and intracellular phenotyping was performed using Canto II (BD Biosciences; San Jose, CA) or NovoCyte flow cytometers (ACEA Biosciences; San Diego, CA). Most antibodies were purchased from BioLegend or Tonbo Biosciences. For intracellular staining of cytokines, cells were stained for surface markers, followed by activation with phorbol 12-myristate 13-acetate (PMA; 50 ng/mL; Sigma Aldrich), ionomycin (1 μg/mL; Sigma Aldrich), and monensin (2 μM; Sigma Aldrich) for 3–4 h. Cells were fixed with 1% paraformaldehyde for at least 2 hours, then permeabilized with saponin buffer and stained for intracellular cytokines. For transcription factor staining, FoxP3 Fix/Perm reagents (Tonbo Biosciences) were used per manufacturer guidelines. Antibodies used for surface markers included CD4 (clone RM4–5), CD8α (clone 53–6.7), CD25 (clone PC61), CD44 (clone IM7), CD90.1 (clone OX-7), and CD3 (clone 17A2). Antibodies for intracellular markers included FoxP3 (eBioscience, clone FJK-16S), IL-17A (clone TC11–18H10.1), and IFNγ (clone XMG1.2).

Flow cytometric analysis of Akt and mTOR activation

For analysis of mTOR activation, S6 phosphorylation (S235/236) was analyzed in cultured naïve T cells in Th17-polarized culture conditions for 1 to 48 h after culture. Akt phosphorylation (S473) was measured in splenocytes cultured in complete RPMI for 16 h in the presence or absence of 10 nM RA, followed by 15 min of activation by anti-CD3/CD28 and hIL-2. Cells were fixed with BD Biosciences Phosflow™ Fix/Perm buffer and permeabilized with BD Phosflow™ Perm III buffer and stained with anti-pAkt (pS473; BD Biosciences), pS6 (pS235/236, Cell Signaling Technology; Danvers, MA), or rabbit IgG isotype (Cell Signaling Technology). When used in combination with retroviral transduction of either RARα or Myr-Akt (Addgene #49267) cells were first cultured overnight with anti-CD3/CD28 activation, retrovirally transduced, and rested for 24 h prior to reactivation with anti-CD3/CD28 and hIL-2 and flow cytometry analysis.

Quantitative RT-PCR analysis for mRNA expression

RNA expression in T cells was assessed by extraction of RNA with Ribosol (VWR, Radnor, PA) and preparation of cDNA with the High Capacity cDNA Reverse Transcription kit (Thermo Fisher). Quantitative RT-PCR was performed using the Maxima SYBR Green/ROX

kit (Thermo Fisher). Expression was normalized to *Actb* (β-actin) and shown as relative to WT levels. Primers are listed in Supplemental Table 1.

Dual luciferase assay of RARE activity

To assess transcriptional activity of RARE sites for validation of RARα activity in mouse strains, naïve T cells were cultured with anti-CD3, anti-CD28, and hIL-2 for 16 hours, then 4×10^6 cells were co-transfected with pGL3-RARE (Addgene #13458) and pRL-CMV (Promega) using the Mouse T Cell Nucleofector kit and Nucleofector 2b device (Lonza; Houston, TX), rested for 4 h in Lonza recovery media with or without 10 nM RA, and restimulated for 6 h with anti-CD3, anti-CD28, and hIL-2 with or without 10 nM RA. Cells were lysed with passive lysis buffer and luminescence of both Renilla and Firefly luciferases were measured using the Dual Luciferase kit (Promega; Madison, WI) on a SpectraMax i3x (Molecular Devices; San Jose, CA) plate reader.

Mitochondrial mass measurement and imaging

In vitro cultures of naïve T helper cells in indicated culture conditions were harvested at 24 h of culture and stained with Mitotracker Green (Thermo Fisher) and assessed by flow cytometry for mitochondrial mass by Mitotracker Green intensity and cell size by forward scatter. Cells from the same cultures were additionally stained with TRITC (Sigma Aldrich) for the cell membrane and DRAQ5 (Thermo Fisher) for DNA, spun onto glass slides, and imaged using a Leica SP5 laser scanning confocal microscope with 63× objective.

Cell proliferation assays

Naïve T helper cells were stained with 2.5 μM CellTrace™ CFSE (Thermo Fisher; Grand Island, NY) and cultured at 1×10^6/mL in a Th17-polarizating condition for 48 h. Proliferation of viable CD4$^+$ cells was assessed by flow cytometry. For XTT assays, naïve T helper cells were cultured at 1×10^6/mL in indicated polarization conditions for 72 h. Proliferation was assessed with the XTT kit (ATCC; Manassas, VA) using absorbance measurements ($A_{450} - A_{690}$) on a Synergy HT (BioTek; Winooski, VT) plate reader following 2-hour incubation of cultures with XTT.

Cell cycle analysis

Naïve T helper cells were cultured at 1×10^6/ml in a Th17-polarizating condition for 48 h. Cells were stained for a viability test with Ghost™ Violet 450 viability dye (Tonbo Biosciences; San Diego, CA) and anti-CD4 followed by fixation in 70% ethanol, treatment with ribonuclease, propidium iodide (PI) staining, and analysis by flow cytometry.

Glucose uptake assay

Naïve T cells were cultured for 24 h with anti-CD3/28 and IL-2. Cells were harvested and resuspended in Seahorse XF base medium (glucose-free) supplemented with 5% FBS. A fluorescent glucose analog 2-deoxy-2-[(7-nitro-2,1,3-benzoxadiazol-4-yl)amino]-D-glucose (2-NBDG) was added at 15 μM concentration, and cells were cultured for 30 m, washed with PBS, stained for CD4 and viability, and analyzed by flow cytometry.

Seahorse live-cell metabolic assays

For analysis of metabolic upregulation following TCR stimulation, naïve T helper cells were isolated and cultured at 5×10^5 cells per well in a Cell-Tak (Corning) coated 24-well plate using XF media containing 25 mM glucose, 2 mM glutamine, and 1 mM pyruvate. Plate was centrifuged (400g for 4 min) and incubated at 37C in an ambient incubator for 30 min prior to metabolic analysis. Metabolic measurements were collected using a Seahorse XFe24 analyzer. Baseline metabolic rates were measured, followed by an injection of mouse T-activator CD3/CD28 dynabeads (2:1 bead to cell ratio; Thermo Fisher) with hIL-2 (100 U/mL) to induce TCR stimulation and cellular activation. Subsequent injections of oligomycin (1 μM) to suppress oxidative phosphorylation and 2-deoxyglucose (50 mM) to suppress glycolysis were used to calculate the glycolysis contribution to metabolism. The ECAR and OCR rates were calculated as the change from baseline readings to the average of the three readings preceding oligomycin injection (~70 min after activation).

Mitochondrial metabolism was tested in 24-hour cultures of naïve T cells in the Th17-polarizing condition in cRPMI containing charcoal-stripped FBS, with or without 10 nM RA. Cells were harvested, washed, and resuspended using XF media (Agilent, Santa Clara, CA; 10 mM glucose, 2 mM glutamine, 1 mM pyruvate, pH 7.4) and 5×10^5 cells per well were added to a Cell-Tak coated 24-well plate. Plate was centrifuged (400g for 4 min) and incubated at 37C in an ambient incubator for 30 min prior to metabolic analysis. A Seahorse XFe24 analyzer with the Mito Stress Test kit (Agilent) was used for analysis.

Western blot analysis

For cell signaling molecules, total CD4^{+} cells were isolated from secondary lymphoid tissues of mice using MojoSort™ magnetic separation (BioLegend). Cells were activated with anti-CD3/28 ± RA (20 nM) or left unactivated for indicated times. Proteins were extracted from cells with a lysis buffer (1% Triton X-100 and 0.1% SDS in PBS) and probed using antibodies for total Akt (9272), pAkt (T308; 244F9), pS6K (T421/S424; CST #9204), PTEN (138G6), and β-actin (clone 13E5), which were purchased from Cell Signaling Technology.

Tagged-RARα expression and imaging

WT or ligand-binding defective (ΔLB, G303E) forms of human RARα [45] with a N-terminal FLAG-tag were cloned into pMSCV-Thy1.1 retroviral vectors. Retroviral supernatants containing viral particles were produced from plasmid-transfected Platinum E cells. Naïve T helper cells were cultured for 16 h in cRPMI with plate-bound anti-CD3 (5 μg/mL) and soluble anti-CD28 (2 μg/mL), then transduced with retroviral supernatants in the presence of polybrene (8 μg/mL) by spin transduction (90 m, 2300 rpm, 32°C). Cells were rested for 1–2 h after transduction, then reactivated in a Th17-polarizing condition with or without 10 nM RA for 20 h. Cells were then harvested and stained for surface Thy1.1 (clone OX-7), fixed with 1% paraformaldehyde for 1 hour, permeabilized with flow cytometry perm buffer (Tonbo Biosciences; San Diego, CA) and stained with BV421 anti-FLAG (BioLegend, clone L5) and DRAQ5. Cells were spun onto Cell-Tak coated glass slides and imaged with a Nikon A1 laser scanning confocal microscope with 60× objective. Cellular localization of FLAG-RARα was analyzed using ImageJ.

Confocal microscopy for proximity ligation assay (PLA) and immunofluorescence

For proximity ligation assay of RARα and Class 1A PI3K (p85 subunit), retroviral transduction of FLAG-RARα into WT T cells was performed, followed by 20 h of culture in the Th17-polarized condition. Cells were stained for CD3 (clone 17A2) and Thy1.1 (clone OX-7), followed by fixation in 1% PFA and permeabilization with Perm buffer (Tonbo). Cells were stained for anti-FLAG (Sigma Aldrich, clone M2) and anti-p85 (Cell Signaling, clone 19H8), followed by incubation with probes and amplification using the DuoLink Red Mouse/Rat PLA kit (Sigma Aldrich). Cells were additionally stained with DAPI and imaged on a Nikon A1 confocal microscope with a 60× objective.

T cell-induced colitis

Naïve T cells were magnetically sorted and 5×10^5 cells per mouse were injected into the retroorbital sinus of Rag1$^{-/-}$ mice in 100 μL PBS. These mice received tap water and Teklad 2018 regular non-autoclaved rodent chow containing 15 IU/g of vitamin A acetate. Mice from different groups were cohoused, with bedding rotated between cages 2–3 times weekly to rule out any microbial differences. Body weight change and stool score were monitored, and mice were euthanized and assessed for intestinal inflammation and T cell phenotyping by flow cytometry on week 5 or when any mice lost more than 20% of body weight. Tissues were processed to prepare single cell suspensions for flow cytometry as previously described.

Statistics

Statistical significance was tested using GraphPad Prism v7.0. Differences between two groups were compared using two-tailed Student's t-test. For three or more groups, one-way ANOVA with Bonferroni's multiple testing correction was used. For comparisons with two factors (e.g. RA and RARα), two-way ANOVA with Bonferroni's multiple testing correction was used. P values <0.05 were considered significant. All error bars indicate SEM.

Supplementary Material

Refer to Web version on PubMed Central for supplementary material.

Acknowledgments

References

1. Wang R et al. The transcription factor Myc controls metabolic reprogramming upon T lymphocyte activation. Immunity 35, 871–882 (2011). [PubMed: 22195744]

2. Hedeskov CJ Early effects of phytohaemagglutinin on glucose metabolism of normal human lymphocytes. Biochem J 110, 373–380 (1968). [PubMed: 5726214]

3. Chapman NM, Boothby MR & Chi H Metabolic coordination of T cell quiescence and activation. Nat Rev Immunol 20, 55–70 (2020). [PubMed: 31406325]

4. Pearce EL & Pearce EJ Metabolic pathways in immune cell activation and quiescence. Immunity 38, 633–643 (2013). [PubMed: 23601682]

5. Frauwirth KA et al. The CD28 signaling pathway regulates glucose metabolism. Immunity 16, 769–777 (2002). [PubMed: 12121659]

6. Dimeloe S, Burgener AV, Grahlert J & Hess C T-cell metabolism governing activation, proliferation and differentiation; a modular view. Immunology 150, 35–44 (2017). [PubMed: 27479920]

7. Ward SG & Cantrell DA Phosphoinositide 3-kinases in T lymphocyte activation. Curr Opin Immunol 13, 332–338 (2001). [PubMed: 11406365]

8. Genot EM et al. The T-cell receptor regulates Akt (protein kinase B) via a pathway involving Rac1 and phosphatidylinositide 3-kinase. Mol Cell Biol 20, 5469–5478 (2000). [PubMed: 10891487]

9. Delgoffe GM et al. The mTOR kinase differentially regulates effector and regulatory T cell lineage commitment. Immunity 30, 832–844 (2009). [PubMed: 19538929]

10. Araki K et al. mTOR regulates memory CD8 T-cell differentiation. Nature 460, 108–112 (2009). [PubMed: 19543266]

11. Ward SG, Westwick J, Hall ND & Sansom DM Ligation of CD28 receptor by B7 induces formation of D-3 phosphoinosites in T lymphocytes independently of T cell receptor/CD3 activation. Eur J Immunol 23, 2572–2577 (1993). [PubMed: 8405057]

12. Gigoux M et al. Inducible costimulator promotes helper T-cell differentiation through phosphoinositide 3-kinase. Proc Natl Acad Sci U S A 106, 20371–20376 (2009). [PubMed: 19915142]

13. Proud CG Regulation of mammalian translation factors by nutrients. Eur J Biochem 269, 5338–5349 (2002). [PubMed: 12423332]

14. Park J et al. Short-chain fatty acids induce both effector and regulatory T cells by suppression of histone deacetylases and regulation of the mTOR-S6K pathway. Mucosal Immunol 8, 80–93 (2015). [PubMed: 24917457]

15. Mucida D et al. Reciprocal TH17 and regulatory T cell differentiation mediated by retinoic acid. Science 317, 256–260 (2007). [PubMed: 17569825]

16. Coombes JL et al. A functionally specialized population of mucosal CD103+ DCs induces Foxp3+ regulatory T cells via a TGF-beta and retinoic acid-dependent mechanism. J Exp Med 204, 1757–1764 (2007). [PubMed: 17620361]

17. Sun CM et al. Small intestine lamina propria dendritic cells promote de novo generation of Foxp3 T reg cells via retinoic acid. J Exp Med 204, 1775–1785 (2007). [PubMed: 17620362]

18. Benson MJ, Pino-Lagos K, Rosemblatt M & Noelle RJ All-trans retinoic acid mediates enhanced T reg cell growth, differentiation, and gut homing in the face of high levels of co-stimulation. J Exp Med 204, 1765–1774 (2007). [PubMed: 17620363]

19. Schambach F, Schupp M, Lazar MA & Reiner SL Activation of retinoic acid receptor-alpha favours regulatory T cell induction at the expense of IL-17-secreting T helper cell differentiation. Eur J Immunol 37, 2396–2399 (2007). [PubMed: 17694576]

20. Schwartz DM et al. Retinoic Acid Receptor Alpha Represses a Th9 Transcriptional and Epigenomic Program to Reduce Allergic Pathology. Immunity 50, 106–120 e110 (2019). [PubMed: 30650370]

21. Kang SG, Lim HW, Andrisani OM, Broxmeyer HE & Kim CH Vitamin A metabolites induce gut-homing FoxP3+ regulatory T cells. J Immunol 179, 3724–3733 (2007). [PubMed: 17785809]

22. Brown CC et al. Retinoic acid is essential for Th1 cell lineage stability and prevents transition to a Th17 cell program. Immunity 42, 499–511 (2015). [PubMed: 25769610]

23. Kang SG, Wang C, Matsumoto S & Kim CH High and low vitamin A therapies induce distinct FoxP3+ T-cell subsets and effectively control intestinal inflammation. Gastroenterology 137, 1391–1402 e1391–1396 (2009). [PubMed: 19632226]

24. Iwata M, Eshima Y & Kagechika H Retinoic acids exert direct effects on T cells to suppress Th1 development and enhance Th2 development via retinoic acid receptors. Int Immunol 15, 1017–1025 (2003). [PubMed: 12882839]

25. Iwata M et al. Retinoic acid imprints gut-homing specificity on T cells. Immunity 21, 527–538 (2004). [PubMed: 15485630]

26. Kang SG, Park J, Cho JY, Ulrich B & Kim CH Complementary roles of retinoic acid and TGF-beta1 in coordinated expression of mucosal integrins by T cells. Mucosal Immunol 4, 66–82 (2011). [PubMed: 20664575]

27. Liu Q & Kim CH Control of Tissue-Resident Invariant NKT Cells by Vitamin A Metabolites and P2X7-Mediated Cell Death. J Immunol 203, 1189–1197 (2019). [PubMed: 31308092]

28. Hashimoto-Hill S, Friesen L, Kim M & Kim CH Contraction of intestinal effector T cells by retinoic acid-induced purinergic receptor P2X7. Mucosal Immunol 10, 912–923 (2017). [PubMed: 27966552]

29. Mark M, Ghyselinck NB & Chambon P Function of retinoid nuclear receptors: lessons from genetic and pharmacological dissections of the retinoic acid signaling pathway during mouse embryogenesis. Annu Rev Pharmacol Toxicol 46, 451–480 (2006). [PubMed: 16402912]

30. Rondina MT et al. Non-genomic activities of retinoic acid receptor alpha control actin cytoskeletal events in human platelets. J Thromb Haemost 14, 1082–1094 (2016). [PubMed: 26848712]

31. Masia S, Alvarez S, de Lera AR & Barettino D Rapid, nongenomic actions of retinoic acid on phosphatidylinositol-3-kinase signaling pathway mediated by the retinoic acid receptor. Mol Endocrinol 21, 2391–2402 (2007). [PubMed: 17595318]

32. Khatib T et al. Genomic and non-genomic pathways are both crucial for peak induction of neurite outgrowth by retinoids. Cell Commun Signal 17, 40 (2019). [PubMed: 31046795]

33. Coyle KM, Maxwell S, Thomas ML & Marcato P Profiling of the transcriptional response to all-trans retinoic acid in breast cancer cells reveals RARE-independent mechanisms of gene expression. Sci Rep 7, 16684 (2017). [PubMed: 29192143]

34. Chen Y, Dokmanovic M, Stein WD, Ardecky RJ & Roninson IB Agonist and antagonist of retinoic acid receptors cause similar changes in gene expression and induce senescence-like growth arrest in MCF-7 breast carcinoma cells. Cancer Res 66, 8749–8761 (2006). [PubMed: 16951191]

35. Piskunov A & Rochette-Egly C A retinoic acid receptor RARalpha pool present in membrane lipid rafts forms complexes with G protein alphaQ to activate p38MAPK. Oncogene 31, 3333–3345 (2012). [PubMed: 22056876]

36. Farrar NR, Dmetrichuk JM, Carlone RL & Spencer GE A novel, nongenomic mechanism underlies retinoic acid-induced growth cone turning. J Neurosci 29, 1413614142 (2009).

37. Koyasu S The role of PI3K in immune cells. Nat Immunol 4, 313–319 (2003). [PubMed: 12660731]

38. Hall JA et al. Essential role for retinoic acid in the promotion of CD4(+) T cell effector responses via retinoic acid receptor alpha. Immunity 34, 435–447 (2011). [PubMed: 21419664]

39. McAdam AJ et al. Mouse inducible costimulatory molecule (ICOS) expression is enhanced by CD28 costimulation and regulates differentiation of CD4+ T cells. J Immunol 165, 5035–5040 (2000). [PubMed: 11046032]

40. Zeng H et al. mTORC1 and mTORC2 Kinase Signaling and Glucose Metabolism Drive Follicular Helper T Cell Differentiation. Immunity 45, 540–554 (2016). [PubMed: 27637146]

41. Saxton RA & Sabatini DM mTOR Signaling in Growth, Metabolism, and Disease. Cell 169, 361–371 (2017).

42. Inoki K, Li Y, Zhu T, Wu J & Guan KL TSC2 is phosphorylated and inhibited by Akt and suppresses mTOR signalling. Nat Cell Biol 4, 648–657 (2002). [PubMed: 12172553]

43. Gullberg M et al. Cytokine detection by antibody-based proximity ligation. Proc Natl Acad Sci U S A 101, 8420–8424 (2004). [PubMed: 15155907]

44. Shi LZ et al. HIF1alpha-dependent glycolytic pathway orchestrates a metabolic checkpoint for the differentiation of TH17 and Treg cells. J Exp Med 208, 1367–1376 (2011). [PubMed: 21708926]

45. Saitou M, Narumiya S & Kakizuka A Alteration of a single amino acid residue in retinoic acid receptor causes dominant-negative phenotype. J Biol Chem 269, 19101–19107 (1994). [PubMed: 7913468]

46. Michalek RD et al. Cutting edge: distinct glycolytic and lipid oxidative metabolic programs are essential for effector and regulatory CD4+ T cell subsets. J Immunol 186, 3299–3303 (2011). [PubMed: 21317389]

47. Chapman NM & Chi H Hallmarks of T-cell Exit from Quiescence. Cancer Immunol Res 6, 502–508 (2018). [PubMed: 29716982]

48. Kane LP & Weiss A The PI-3 kinase/Akt pathway and T cell activation: pleiotropic pathways downstream of PIP3. Immunol Rev 192, 7–20 (2003). [PubMed: 12670391]

49. Shim EK, Jung SH & Lee JR Role of two adaptor molecules SLP-76 and LAT in the PI3K signaling pathway in activated T cells. J Immunol 186, 2926–2935 (2011). [PubMed: 21282515]

50. Hay N Interplay between FOXO, TOR, and Akt. Biochim Biophys Acta 1813, 1965–1970 (2011). [PubMed: 21440577]

51. Frota-Ruchon A, Marcinkiewicz M & Bhat PV Localization of retinal dehydrogenase type 1 in the stomach and intestine. Cell Tissue Res 302, 397–400 (2000). [PubMed: 11151452]

52. Hashimoto-Hill S et al. RARalpha supports the development of Langerhans cells and langerin-expressing conventional dendritic cells. Nat Commun 9, 3896 (2018). [PubMed: 30254197]

53. Bhattacharya N et al. Normalizing Microbiota-Induced Retinoic Acid Deficiency Stimulates Protective CD8(+) T Cell-Mediated Immunity in Colorectal Cancer. Immunity 45, 641–655 (2016). [PubMed: 27590114]

54. Zhumabekov T, Corbella P, Tolaini M & Kioussis D Improved version of a human CD2 minigene based vector for T cell-specific expression in transgenic mice. J Immunol Methods 185, 133–140 (1995). [PubMed: 7665895]

55. Chapellier B et al. A conditional floxed (loxP-flanked) allele for the retinoic acid receptor alpha (RARalpha) gene. Genesis 32, 87–90 (2002). [PubMed: 11857786]

Author Manuscript

Author Manuscript

Author Manuscript

Author Manuscript
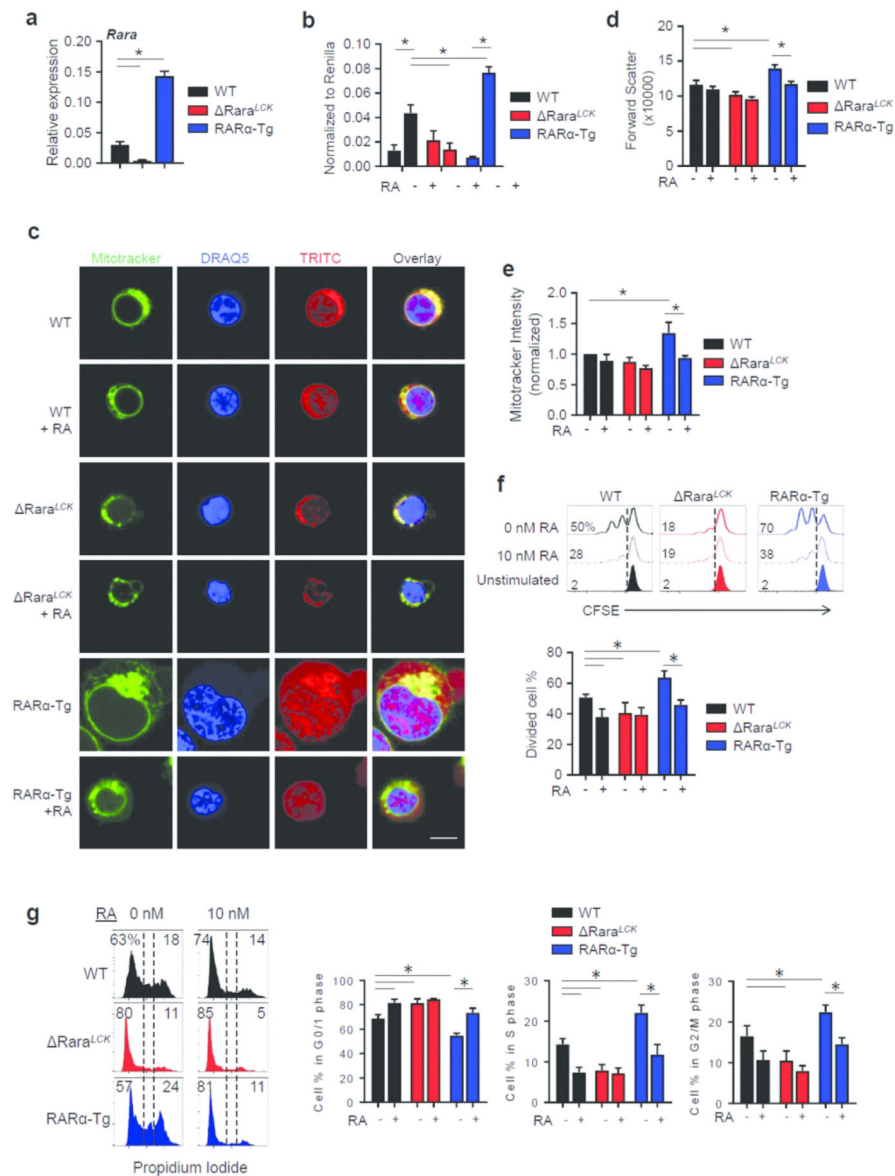
Fig. 1. The dose effect of RARα on cell size, proliferation, and mitochondrial mass.
(a) Expression levels of full length RARα mRNA in naïve CD4^{+} T cells isolated from the spleen of WT, Rara^{LCK}, and RARα-Tg mice. (b) RARE-reporter activity in WT, Rara^{LCK}, and RARα-Tg T helper cells. (c) Cell size, morphology, and mitochondrial staining at 24 h during activation. Scale bar is 5 μm. (d) Cell size of WT, Rara^{LCK}, and RARα-Tg CD4 T cells, based on forward scatter characteristics at 24 h during activation. (e) Mitotracker staining for mitochondrial content in CD4^{+} T cells. (f) Cell proliferation as measured by CFSE dilution at 48 h during activation. (g) Cell cycle analysis based on PI staining at 48 h of activation. (c-g) Naïve CD4^{+} T cells were cultured in a Th17-polarization condition (mIL-6, mIL-1ß, mIL-21, mIL-23, mTNFα, hTGFβ–1, anti-IFNγ, and anti-IL-4) for indicated periods. Representative and combined data (n=6 for a; n=3 for b-f; n=4 for g) are shown. All error bars indicate SEM. *Significant differences (P values <0.05) between
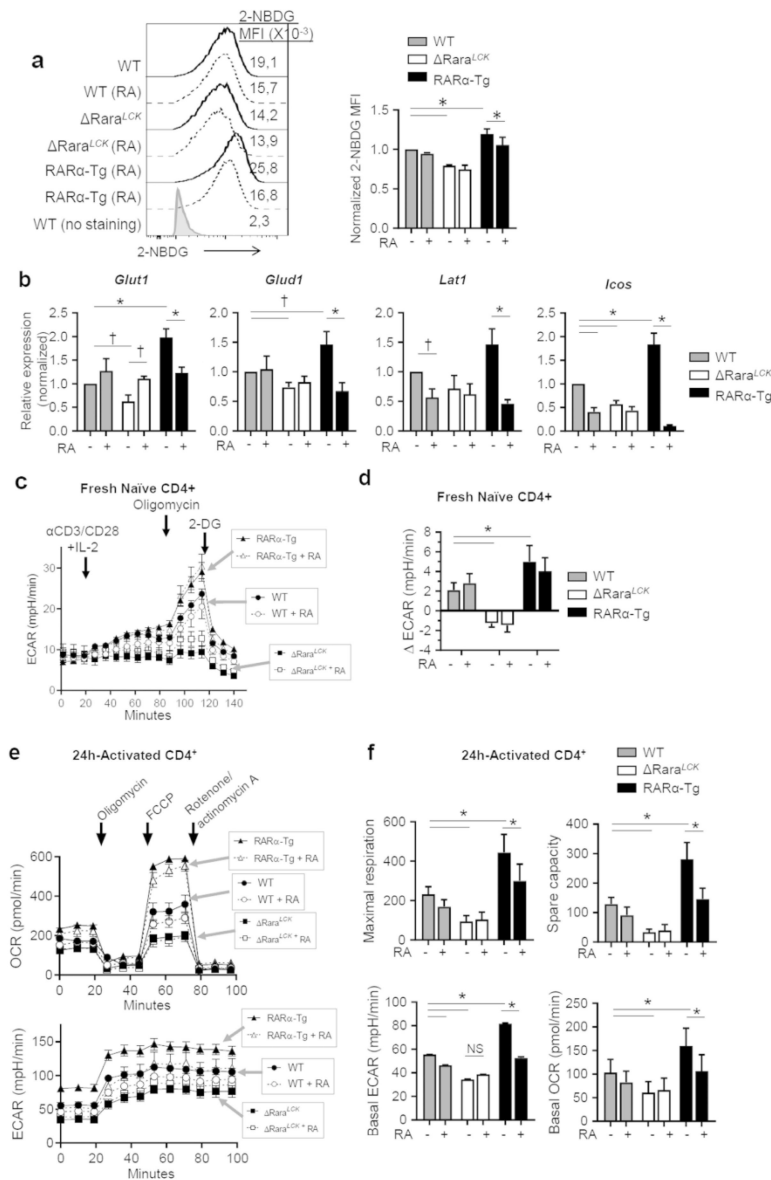
indicated groups by repeated-measures two-way ANOVA with Bonferroni. For panel a, one-way ANOVA with Bonferroni was used.

Fig. 2. RARα invigorates cell metabolism in T cells during activation.
(a) Glucose uptake measured in 24 h activated cells with anti-CD3/28 and IL-2. (b) RNA expression of metabolism-linked genes in 24 h activated cells. (c) Seahorse assay ECAR measurements of naïve CD4+ T cells upon anti-CD3/CD28 and IL-2 stimulation. (d) Changes in ECAR (ECAR) during the first ~70 m period following activation. (e) Mitochondrial stress test for OCR and ECAR in cultured naïve CD4+ T cells after 24 h activation. In panels b, e and f, naïve CD4+ T cells were cultured in a Th17-polarization condition for 24 h prior to metabolic measurements. Representative and combined data (n=3 for a; n=3–8 for b; n=3 for c-f) are shown. All error bars indicate SEM. *Significant differences (*P* values <0.05) from control or between two groups analyzed by repeated-measures two-way ANOVA with Bonferroni, except for significance (†) measured by two-tailed t-test in panel b.
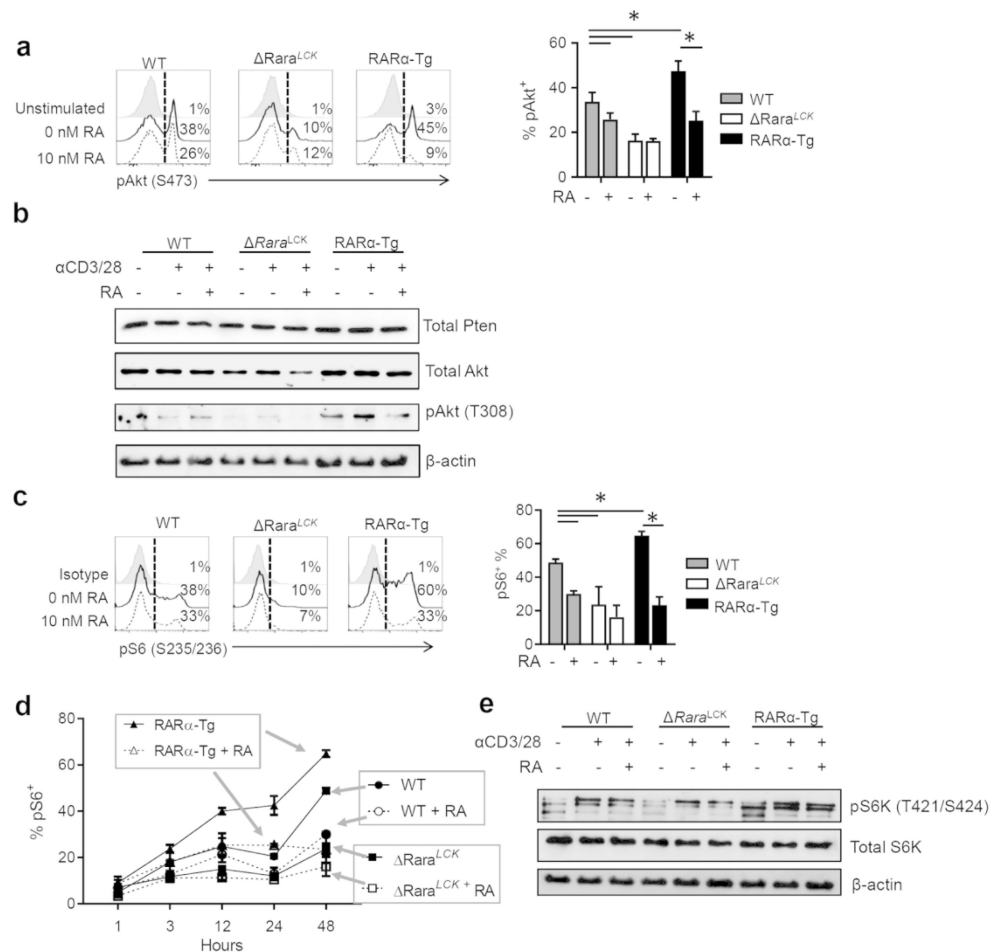
Fig. 3. RARα positively regulates the activity levels of Akt and mTOR in CD4$^+$ T cells.
(a) Activation of Akt1/2/3 (S473 phosphorylation) in WT, Rara^{LCK}, and RARα-Tg CD4 T cells. (b) Expression of Pten and Akt and phosphorylation of pAkt (T308). (c) Activation of mTOR based on rS6 phosphorylation (Ser 235/236) in WT, Rara^{LCK}, and RARα-Tg CD4 T cells. (d) Kinetics of rS6 phosphorylation in WT, Rara^{LCK}, and RARα-Tg CD4 T cells in 48 h period. (e) Phosphorylation of rS6K (T421/S424). Splenocytes (a,c,d) or total CD4$^+$ T (b,e) cells were activated in a Th17 cell cytokine condition with anti-CD3 and CD28 in the presence or absence of RA (10–20 nM) for 15 min (a), 48 h (c), or indicated times (d). Combined and representative data from more than 4 independent experiments are shown. *Significant differences (P values <0.05) between indicated groups analyzed by repeated-measures two-way ANOVA with Bonferroni.
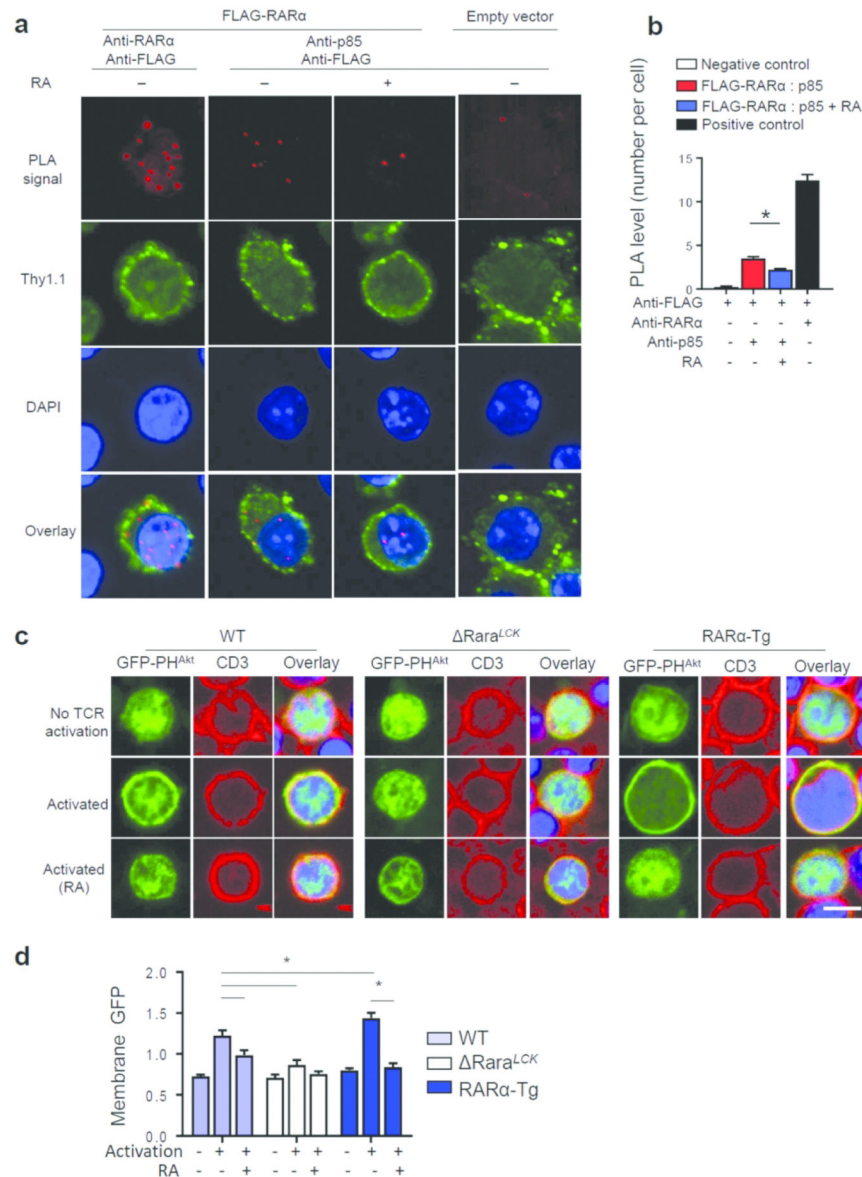
Fig. 4. Association between RARα to PI3K and its impact on phosphatidylinositol-3, 4, 5-triphosphate (PIP$_3$) generation in the cellular membrane of CD4$^+$ T cells.
(a) Proximity ligation assay of p85 and FLAG-RARα in retrovirally-transduced CD4$^+$ T cells. Negative control lacks FLAG-RARα; positive control uses monoclonal anti-RARα antibody and anti-FLAG antibody. (b) Quantified PLA levels, indicating RARα association with p85. (c, d) Detection of PIP$_3$, an enzymatic product of PI3K, in T cells utilizing GFP-PH^{Akt}. CD4 T cells were transfected with a plasmid expressing GFP-PH^{Akt} and activated for 15 min followed by paraformaldehyde fixation, anti-CD3 and DRAQ5 staining, and confocal microscopy. Combined and representative data (n=4 for a, b, n=3–4 for c, d) are shown. *Significant differences (P values <0.05) from indicated groups by one-way ANOVA with Bonferroni (b) or two-way ANOVA with Bonferroni (d).
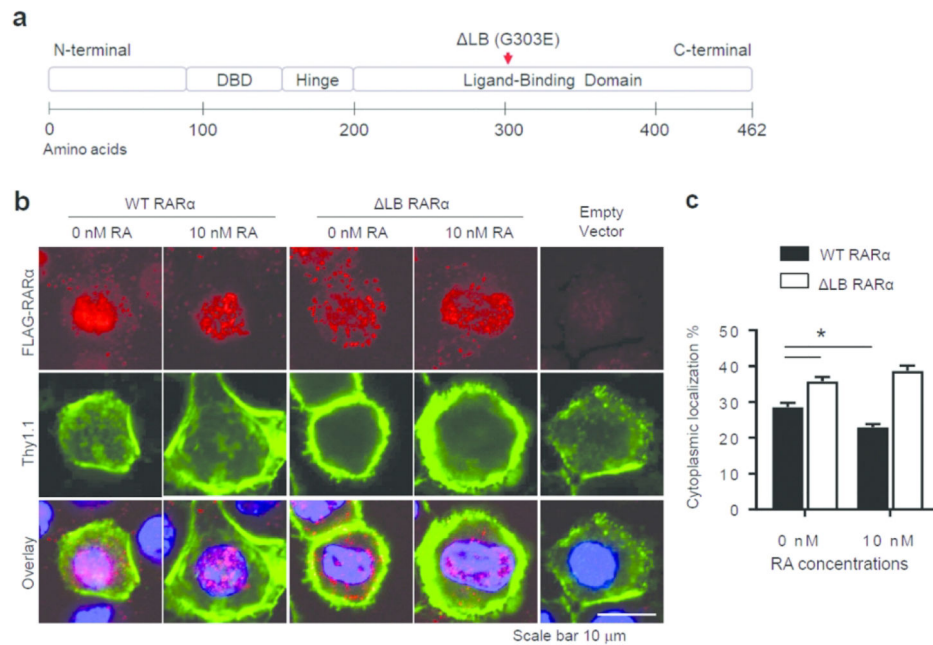
Fig. 5. Impact of RA and ligand binding ability on nuclear versus cytoplasmic RARα localization.

(a) Domains and the mutation site for G303E in the RARα protein. (b) Confocal images of FLAG-RARα expressed in CD4+ T cells. FLAG-RARα was expressed in CD4+ T cells by retroviral gene transfer. Naïve CD4+ T cells were activated overnight and transduced with recombinant retrovirus particles and further cultured in a Th17 cell cytokine condition for 16h without or with RA (10 nM). (c) Cytoplasmic localization of FLAG-RARα as a percentage of total cell signal was measured using ImageJ. *Significant differences (*P* values <0.05) from indicated groups by two-way ANOVA with Bonferroni (c).
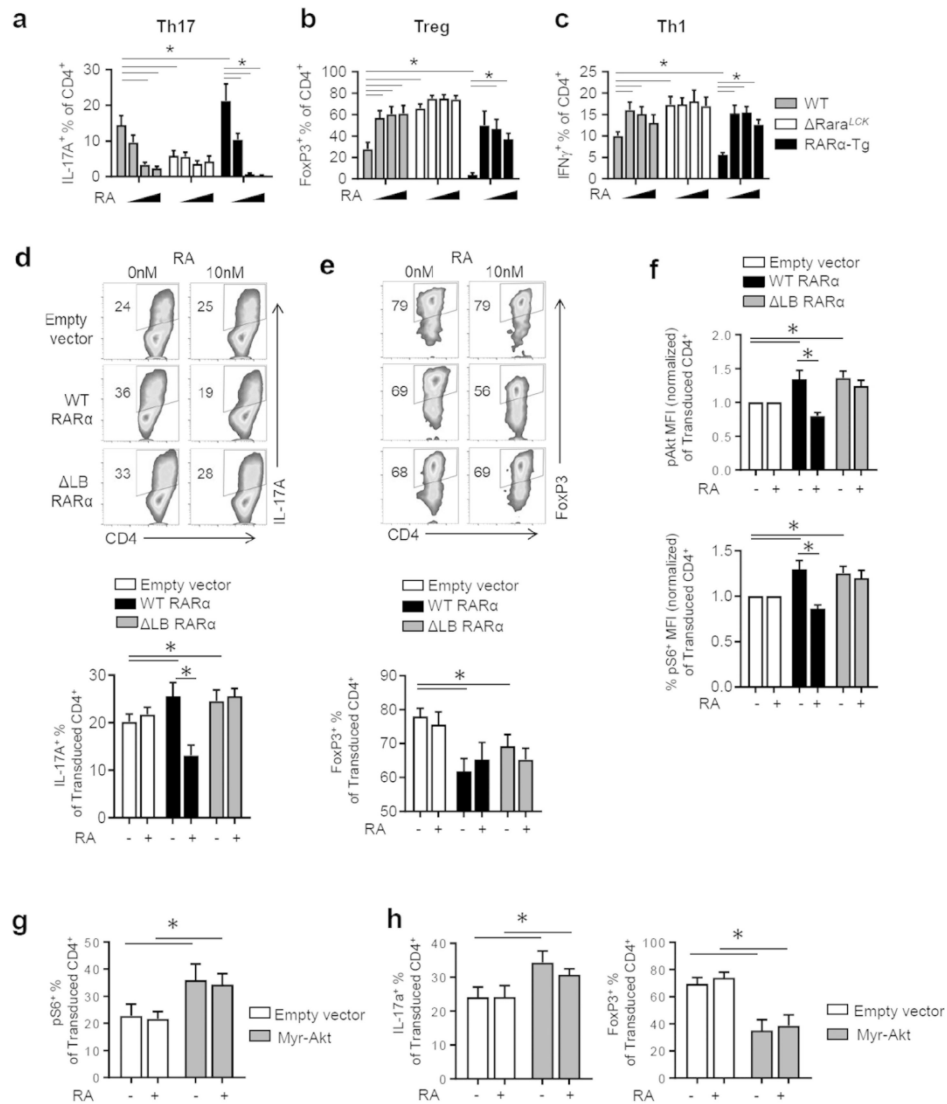
Fig. 6. Gain and loss of function effects of RARα on T cell differentiation and Akt/mTOR activity.

(a-c) Impact of RARα dose and RA (0, 1, 10, 50 nM) on Th17/Treg/Th1 polarization *in vitro.* (d) Impact of the expression of WT and LB RARα on the polarization of naive Rara^{LCK} CD4 T cells into Th17 cells. (e) Impact on the polarization of naive Rara^{LCK} CD4 T cells into FoxP3$^+$ T cells. (f) Impact on the phosphorylation of Akt (S473) and rS6 (S235/236) in Rara^{LCK} CD4 T cells. (g) Impact of the constitutively active form of Akt (Myr-Akt) on mTOR activation (rS6 phosphorylation). (h) Impact of Myr-Akt on Th17 versus Treg differentiation. For panel d, e, and h, Rara^{LCK} T helper cells were transduced after 16 h culture with anti-CD3/CD28 (5 μg/mL and 2 μg/mL, respectively) with RARα- or Myr-Akt-expressing retrovirus and subsequently cultured in Th17- or Treg-polarizing culture for 3 additional days prior to flow cytometry analysis. For panels f and g, Rara^{LCK} T helper cells were similarly transduced and cultured in Th17-polarizing culture for 20 h prior to flow cytometry analysis. Representative and combined data (n=4–7) from more than

4 independent experiments are shown. *Significant differences (P values <0.05) between indicated groups by repeated measures two-way ANOVA with Bonferroni.
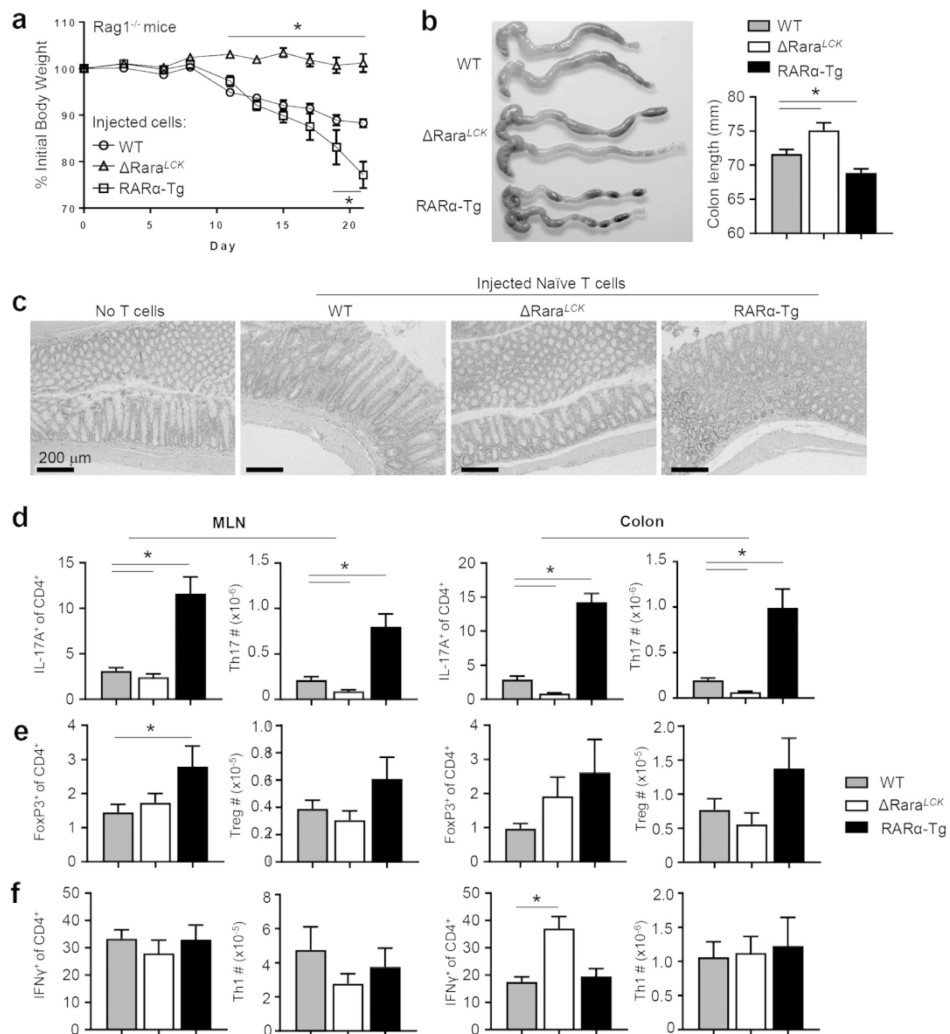
Fig. 7. The dose effect of RARα on Th differentiation in an inflammatory condition.
(a) WT, Rara^{LCK}, and RARα-Tg naïve CD4 T cells were transferred into Rag1$^{-/-}$ mice, and weight change was monitored. (b) Colon length at termination. (c) Histological examination of the distal colon. Impact of RARα dose on Th17 (d), Treg (e) and Th1 (f) activity in Rag1$^{-/-}$ mice. Representative and combined data (n=12–18) from 3–4 independent experiments are shown. *Significant differences (*P* values <0.05) between indicated groups by one-way ANOVA with Bonferroni.